



1,6- and 1,7-regioisomers of dinitro- and diamino-substituted perylene bisimides: synthesis, photophysical and electrochemical properties

Hsing-Yang Tsai, Che-Wei Chang, Kew-Yu Chen *

Department of Chemical Engineering, Feng Chia University, 40724 Taichung, Taiwan, ROC



ARTICLE INFO

Article history:

Received 30 September 2013

Revised 2 December 2013

Accepted 10 December 2013

Available online 19 December 2013

Keywords:

1,6-Dinitroperylene bisimide

1,6-Diaminoperylene bisimide

Intramolecular charge transfer

Lippert–Mataga equation

ABSTRACT

1,6- and 1,7-regioisomers of dinitro- (**1,6-3** and **1,7-3**) and diamino-substituted perylene bisimides (**1,6-1** and **1,7-1**) were synthesized. The regioisomers **1,6-3** and **1,7-3** were successfully separated by high performance liquid chromatography and characterized by 500 MHz ¹H NMR spectroscopy. Subsequently, the reduction of **1,6-3** and **1,7-3** afforded the corresponding diaminoperylene bisimides **1,6-1** and **1,7-1**, respectively. This is the first time 1,6-regioisomers of dinitro- and diamino-substituted perylene bisimides are obtained in pure form. The photophysical and electrochemical properties of **1,6-3** and **1,7-3** were found to be almost the same. However, the regioisomers **1,6-1** and **1,7-1** exhibit significant differences in their optical characteristics. The absorption spectrum of **1,6-1** covers a larger part of the visible region compared to that of **1,7-1**. Upon excitation, **1,6-1** also show larger dipole moment change than that of **1,7-1**. Time-dependent density functional theory calculations are reported on these dyes in order to rationalize their electronic structure and absorption spectra.

© 2013 Elsevier Ltd. All rights reserved.

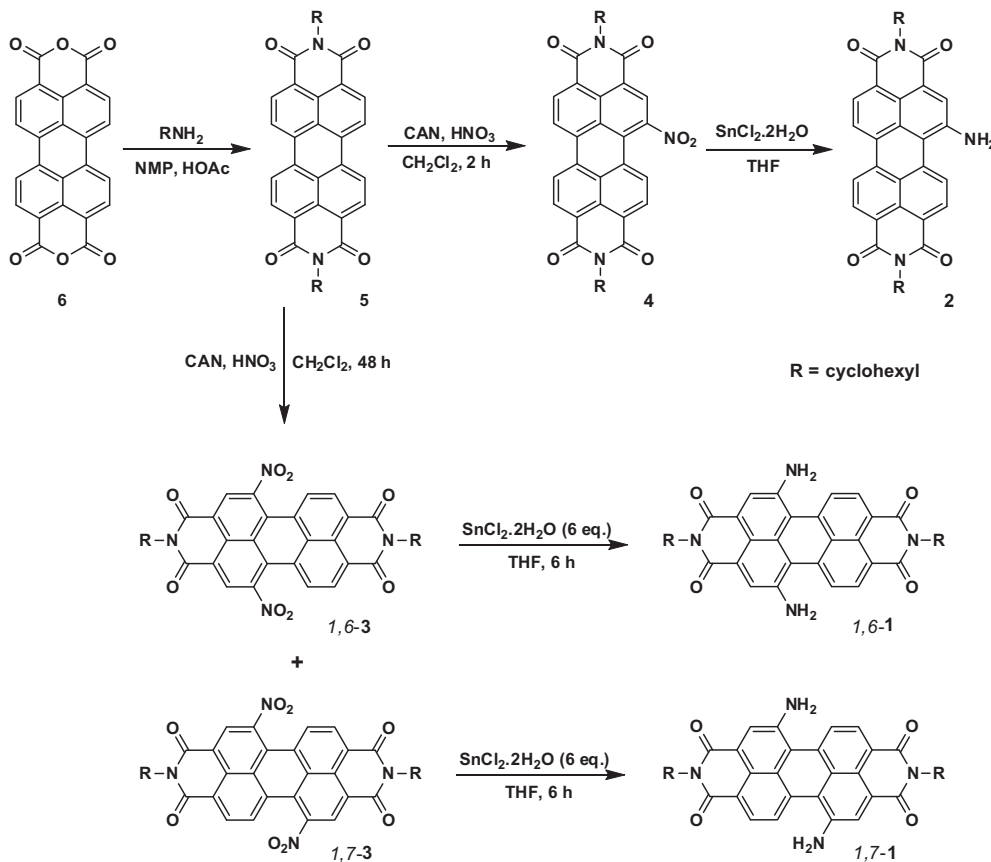
Perylene bisimides (PBIs) and related derivatives possess excellent thermal, photochemical and photophysical stabilities with high extinction coefficients.¹ Their use has been explored for potential applications in molecular electronic and optical devices, such as photovoltaic cells,² light-emitting diodes,³ organic field-effect transistors (OFETs),⁴ dye lasers,⁵ optical power limiters,⁶ LCD color filters,⁷ light-harvesting arrays,⁸ electrophotographic devices,⁹ photochromic materials,¹⁰ logic gates,¹¹ and molecular wires.¹² They have also been utilized as building blocks to construct supramolecular or artificial photosynthetic systems.¹³ In recent years, more and more novel perylene bisimide derivatives with either electron-donating or electron-withdrawing groups were reported in the literature, such as (a) piperidinyl-substituted PBIs,¹⁴ (b) pyrrolidinyl-substituted PBIs,¹⁵ (c) alkylamino-substituted PBIs,¹⁶ (d) amino-substituted PBIs,¹⁷ (e) alkoxy-substituted PBIs,¹⁸ (f) hydroxy-substituted PBIs,¹⁹ (g) aryl-substituted PBIs,²⁰ (h) ferrocenyl-substituted PBIs,²¹ (i) alkyl-substituted PBIs,²² (j) perfluoroalkyl-substituted PBIs,²³ (k) boryl-substituted PBIs,²⁴ (l) cyano-substituted PBIs,²⁵ (m) nitro-substituted PBIs,²⁶ etc. To date, a general method for introducing substituents onto the PBIs' core is bromination or chlorination of perylene-3,4,9,10-tetracarboxylic dianhydride (**6**). Nucleophilic substitutions and metal-catalyzed

cross-coupling reactions can then be executed and yield a regioisomeric mixture of 1,6- and 1,7-disubstituted PBIs. The most widely reported molecules made from the above reaction were 1,7-disubstituted PBIs,²⁷ rather than 1,6-disubstituted PBIs.^{14a} Recently, Dubey et al. have synthesized, separated, and characterized 1,6- and 1,7-regioisomers of diphenoxyl and dipyrrolidinyl substituted PBIs.²⁸ The results have shown that 1,6-dipyrrolidinylperylene bisimide covers a larger portion of the visible region (450–750 nm) compared to that of 1,7-dipyrrolidinylperylene bisimide. Therefore, the 1,6-regioisomer may be of particular interest for organic photovoltaic applications. To expand the scope of the PBI-based dyes available for designing systems for OFETs and photovoltaic cells, the present research reports the synthesis, separation, characterization, photophysical and electrochemical properties of 1,6- and 1,7-regioisomers of dinitro- and diamino-substituted PBIs.

Scheme 1 shows the chemical structures and synthetic routes of nitro-substituted (**3** and **4**) and amino-substituted PBIs (**1** and **2**). The synthesis starts from an imidization of perylene-3,4,9,10-tetracarboxylic dianhydride (**6**) by reacting with cyclohexylamine. The nitration of perylene bisimide can then be achieved by the reaction of **5** with cerium (IV) ammonium nitrate (CAN) and HNO₃ under ambient temperature. Both mono- and di-substituted nitroperylene bisimides (**4** and **3**) were obtained by controlling the reaction time,²⁹ and the regioisomeric 1,6- and 1,7-dinitroperylene bisimides (**1,6-3** and **1,7-3**) were successfully separated by high

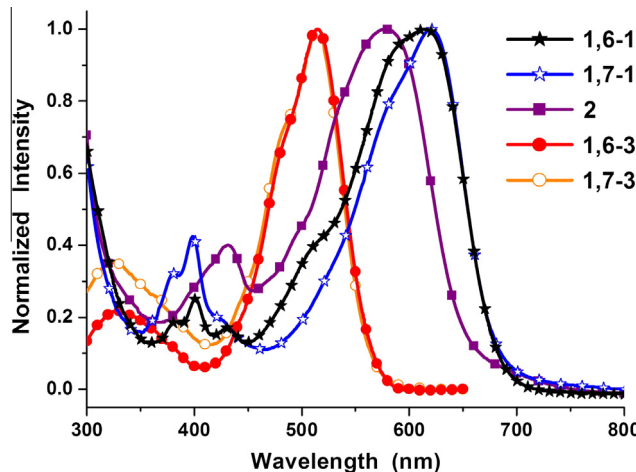
* Corresponding author. Tel.: +886 4 24517250x3683; fax: +886 4 24510890.

E-mail address: kyuchen@fcu.edu.tw (K.-Y. Chen).

**Scheme 1.** Synthetic routes of **1–4**.

performance liquid chromatography (HPLC). Subsequently, the reduction of **1,6-3** and **1,7-3** by tin (II) chloride dihydrate ($\text{SnCl}_2 \cdot 2\text{H}_2\text{O}$) in refluxing THF obtained the 1,6- and 1,7-diaminoperylene bisimides (**1,6-1** and **1,7-1**), respectively.³⁰ It is to be noted that the characteristic signals of the regiosomers **1,6-3** and **1,7-3** in the ^1H NMR spectra (Fig. S1), one singlet and two doublets of perylene core protons, exhibit very small differences in the chemical shift values (0.01 and 0.04 ppm for the doublets at 8.26–8.68). However, a convenient unequivocal assignment of the NMR spectrum to the individual regiosomers **1,6-3** and **1,7-3** was performed on the basis of the signal of methanetriyl protons next to the imide nitrogen at 5.01 ppm. Because of the same chemical environment, both methanetriyl protons of major regiosomer **1,7-3** appear as one common multiplet at 5.01 ppm, but the signal splits into double multiplets for minor regiosomer **1,6-3**. In this way, an unambiguous characterization has been made successfully on the basis of 500 MHz ^1H NMR.

Figure 1 shows the steady state absorption spectra of **1–3** in dichloromethane. The longest wavelength absorption band of both **1,6-3** and **1,7-3** appears at 515 nm, which is assigned to the $\pi-\pi^*$ transitions localized on the perylene core.^{26a} In addition, the absorption spectra of all nitro-substituted PBIs (**1,6-3**, **1,7-3** and **4**) are nearly identical with the spectrum of the non-substituted perylene bisimide (**5**), but they are non-fluorescent chromophores. On the other hand, the reduction of **1,6-3** (**1,7-3**) to **1,6-1** (**1,7-1**) switches the substituent from an electron-withdrawing group to an electron-donating group and causes a large red shift. The spectra of monoamino-substituted (**2**) and diamino-substituted PBIs (**1,6-1** and **1,7-1**) are dominated by very broad absorption bands that span a large part of the visible spectrum (400–750 nm). These broad bands are characteristic of perylene bisimide derivatives

**Figure 1.** Normalized absorption spectra of **1–3** in dichloromethane solution.

N-substituted at the bay-core positions, due to charge transfer absorption.³¹ In contrast to **1,6-3** and **1,7-3**, the diamino-substituted PBIs **1,6-1** and **1,7-1** display significant differences in their absorptive features. In the case of **1,7-1**, the longest wavelength absorption band is centered at 620 nm. Whereas for regiosomer **1,6-1**, this lowest energy band is slightly broader and blue-shifted by ca. 6 nm with respect to that of **1,7-1** and has a small shoulder at ca. 520 nm. The longest wavelength absorption band of both **1,6-1** and **1,7-1** is red-shifted relative to that of the mono-substituted compound (**2**: 578 nm), which can be explained by the fact that the

addition of amino (electron-donating) groups at the perylene core increases the HOMO energy level and hence decreases the energy gap. This viewpoint can be further supported by a theoretical approach based on density functional theory (vide infra). Moreover, the longest wavelength absorption band of **1,6-1** and **1,7-1** exhibits a red shift when the solvent polarity increases (Table 1), which is consistent with previous studies.³¹

The fluorescence spectra of **1,6-1** in various solvents with different polarity are shown in Figure 2 and summarized in Table 1, whereas those of **1,7-1** and **2** can be found in the Supplementary data (Figs. S2 and S3). Unlike the small shift in absorption spectra, the fluorescence spectra of amino-substituted PBIs (**1** and **2**) are largely red-shifted along with the increase of the solvent polarity, which indicates strong intramolecular charge transfer (ICT) characteristics for the excited states of **1,6-1**, **1,7-1** and **2**. We used the well-established fluorescence solvatochromic shift method³² to measure the stabilization of the excited states of **1,6-1** and compared these results to those of **1,7-1** and **2**. The change of magnitudes for dipole moments between ground and excited states, that is, $\Delta\mu = |\overrightarrow{\mu_e} - \overrightarrow{\mu_g}|$, can be calculated by the Lippert–Mataga equation and expressed as:

$$\bar{v}_a - \bar{v}_f = \frac{2}{hc} (\mu_e - \mu_g)^2 a_0^{-3} \Delta f + \text{const.} \quad (1)$$

where h is the Planck constant, c is the speed of light, and a_0 denotes the cavity radius in which the solute resides, calculated to be 7.0 Å via Hartree–Fock theories with 6-31G(d,p') basis, $\bar{v}_a - \bar{v}_f$ is the Stokes shift of the absorption and emission peak maximum, and Δf is the orientation polarizability defined as:

$$\Delta f = f(\epsilon) - f(n^2) = \frac{\epsilon - 1}{2\epsilon + 1} - \frac{n^2 - 1}{2n^2 + 1} \quad (2)$$

The plot of the Stokes shift $\bar{v}_a - \bar{v}_f$ as a function of Δf is sufficiently linear for **1,6-1**, **1,7-1** and **2** (Fig. 2). Accordingly, $\Delta\mu = |\overrightarrow{\mu_e} - \overrightarrow{\mu_g}|$ was calculated to be 5.2 D, 6.1 D and 7.4 D for **1,7-1**, **1,6-1** and **2**, respectively. These values indicate that the asymmetric compound **2** has a larger dipole moment change than that of the symmetric compound **1,6-1** (**1,7-1**), which are in good agreement with previous Letters.³³ The results also show that **1,6-1** (6.1 D) has a larger dipole moment change than that of **1,7-1** (5.2 D). By combining the ¹H NMR spectral data (vide supra) with the $\Delta\mu$ data, we may conclude that the chemical structure of **1,6-1** is more asymmetric than that of **1,7-1**.

The cyclic voltammograms of **1–3** are illustrated in Figure 3. The two regioisomers of dinitro-substituted PBIs (**1,6-3** and **1,7-3**), which are mainly known for their electron-accepting capabilities, showed very similar redox characteristics. Both the isomers exhibit two quasi-reversible one-electron reductions; these are –0.09 and –0.34 V for **1,7-3** and –0.11 and –0.37 V for **1,6-3**. On the other hand, the amino-substituted PBIs (**1,6-1**, **1,7-1** and **2**), which are mainly known for their electron-donating capabilities, undergo two quasi-reversible one-electron oxidations and two quasi-reversible one-electron reductions in dichloromethane at modest potentials. It is apparent that both the first oxidation and the first

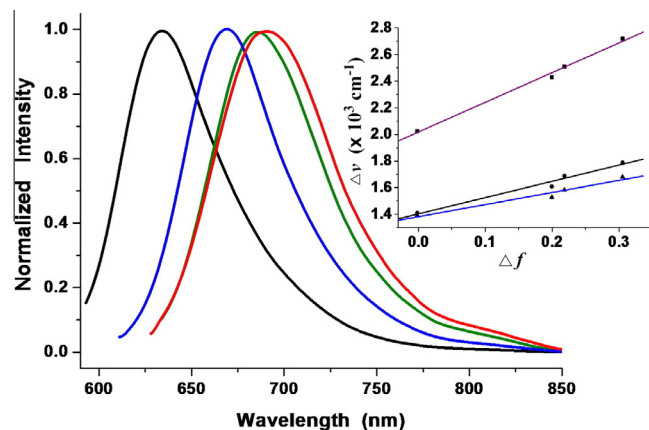


Figure 2. Normalized emission spectra of **1,6-1** in cyclohexane (black line), ethyl acetate (blue line), dichloromethane (green line), and acetonitrile (red line). Lippert–Mataga plots (inset) for **1,6-1** (black line), **1,7-1** (blue line), and **2** (purple line).

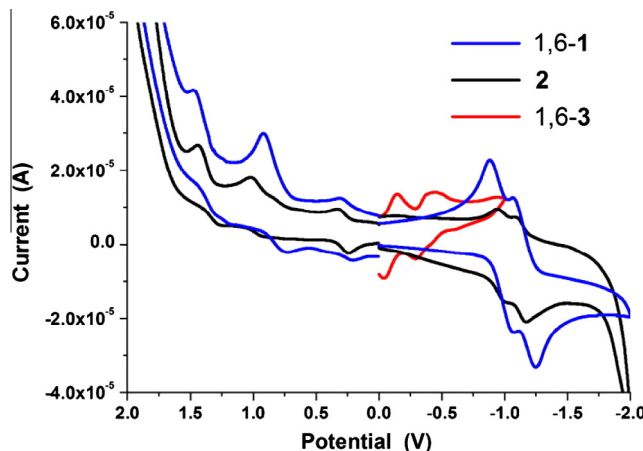


Figure 3. Cyclic voltammograms of **1–3** measured in dichloromethane solution with ferrocenium/ferrocene, at 200 mV/s.

reduction potentials are shifted toward more negative values with increasing numbers of substituted amino groups. The two reversible one-electron oxidations of **1,7-1** occur at 0.79 and 1.17 V, whereas for **1,6-1**, both first and second oxidations are slightly shifted to more positive values by 0.05 and 0.07 V, respectively. The results clearly indicate that the removal of electrons from **1,6-1** is more difficult in comparison to **1,7-1**; these findings are in good agreement with previous reports.²⁸ Table 2 summarizes the redox potentials and the HOMO and LUMO energy levels estimated from cyclic voltammetry (CV) for **1–5**. It appears that the

Table 2
Summary of half-wave redox potentials, HOMO and LUMO energy levels for **1–5**

Compound	$E^{+}_{1/2}$ ^a	$E^{2+}_{1/2}$ ^a	$E^{-}_{1/2}$ ^a	$E^{2-}_{1/2}$ ^a	$E_{\text{HOMO}}/E_{\text{LUMO}}$ (eV) ^b
1,6-1	0.84	1.24	–1.13	–1.23	–5.44/–3.31
1,7-1	0.79	1.17	–1.15	–1.24	–5.39/–3.28
2	0.97	1.36	–0.97	–1.09	–5.57/–3.33
1,6-3	–	–	–0.11	–0.37	–6.73/–4.33
1,7-3	–	–	–0.09	–0.34	–6.75/–4.35
4	–	–	–0.19	–0.51	–6.64/–4.25
5	–	–	–0.46	–0.76	–6.36/–3.98

^a Measured in a solution of 0.1 M tetrabutylammonium hexafluorophosphate (TBAPF₆) in dichloromethane versus SCE (in V).

^b Calculated from $E_{\text{HOMO}} = -4.88 - (E_{\text{oxd}} - E_{\text{Fc/Fc}^+})$, $E_{\text{LUMO}} = E_{\text{HOMO}} + E_g$.

Table 1

Summary of optical absorption and emission properties of **1,6-1** and **1,7-1** in various solvents

1,6-1/1,7-1	λ_{abs} ^a (nm)	λ_{em} (nm)	Φ ^b
Cyclohexane	582/587	634/638	0.15/0.18
Ethyl acetate	604/613	669/675	0.11/0.13
Dichloromethane	612/620	681/693	0.07/0.09
Acetonitrile	615/624	692/701	0.04/0.04

^a Measured at 2×10^{-5} M.

^b Determined with *N,N*-diethyl-3,4,9,10-perylenedicarboximide as reference.^{13b}

first reduction (oxidation) potential is shifted toward a more positive (negative) value with increasing numbers of substituted nitro (amino) groups, while both the HOMO and LUMO energy levels decrease (increase) with the trend. The HOMO/LUMO energy levels of **1,6-1**, **1,7-1**, **2**, **1,6-3** and **1,7-3** are estimated to be $-5.44/-3.31$, $-5.39/-3.28$, $-5.57/-3.33$, $-6.73/-4.33$ and $-6.75/-4.35$ eV, respectively. As a result, the trend of the HOMO–LUMO energy gap is **3** > **2** > **1**, which is in good agreement with the theoretical calculations (vide infra).

For a deeper insight into the molecular structures and electronic properties of **1–5**, quantum chemical calculations were performed using density functional theory (DFT) at the B3LYP/6-31G** level. The highest occupied molecular orbitals (HOMOs) and the lowest unoccupied molecular orbitals (LUMOs) of **1,6-1**, **1,7-1** and **2** are shown in Figure S5. The HOMO of all amino-substituted PBIs (**1,6-1**, **1,7-1** and **2**) is delocalized mainly on the amino group and the perylene core, while the LUMO is extended from the central perylene core to the bisimide groups. The calculated and experimental parameters for perylene bisimide derivatives **1–5** are summarized in Table 3. The results indicate that both the HOMO and LUMO energy levels increase (decrease) as the number of amino (nitro) groups increases, and the calculated band gap energies are in good agreement with experimental data. The absorption and emission spectra of **1,6-1**, **1,7-1** and **2** were also calculated by time-dependent DFT calculations (Franck–Condon principle, Table S1). The calculated excitation/fluorescence wavelengths for the $S_0 \rightarrow S_1/S_1 \rightarrow S_0$ transitions are 558/633 nm for **1,6-1**, 579/646 nm for **1,7-1**, and 547/616 nm for **2**, which is very close to the experimental results. Furthermore, DFT (B3LYP/6-31G**) calculations show that the ground-state geometries of the perylene core have two core twist angles, that is, approximate dihedral angles between the two naphthalene subunits attached to the central benzene ring; these are ~ 20.09 and $\sim 20.10^\circ$ for **1,6-1**, ~ 19.20 and $\sim 19.38^\circ$ for **1,7-1**, ~ 9.18 and $\sim 17.46^\circ$ for **2**, ~ 17.22 and $\sim 17.34^\circ$ for **1,6-3**, ~ 17.02 and $\sim 17.12^\circ$ for **1,7-3**, and ~ 7.89 and $\sim 15.87^\circ$ for **4** (Table 3 and Fig. S6). The core twist angles of the amino-substituted (1,6-disubstituted) PBIs are generally larger than those of nitro-substituted (1,7-disubstituted) compounds.

In summary, we have successfully synthesized, separated, and characterized 1,6- and 1,7-regioisomers of dinitro- and diamino-substituted PBIs. The regioisomers of dinitro-substituted PBIs were separated by conventional high performance liquid chromatography. Subsequently, the reduction of 1,6- and 1,7-dinitroperylene bisimides (**1,6-3** and **1,7-3**) afforded the corresponding diaminoperylene bisimides **1,6-1** and **1,7-1**, respectively. To our best knowledge, this is the first time 1,6-regioisomers of dinitro- and diamino-substituted PBIs are obtained in pure form. Our studies have also shown that these 1,6- and 1,7-isomers can readily be characterized by 500 MHz ^1H NMR. The photophysical and electrochemical properties of **1,6-3** and **1,7-3** were found to be virtually the same. However, the diamino-substituted regioisomers **1,6-1** and **1,7-1** exhibit sig-

nificant differences in their optical characteristics. In addition to the longest wavelength absorption band at around 620 nm, **1,6-1** exhibits another shoulder band at ca. 520 nm, and consequently, covers a large part of the visible region relative to that of **1,7-1**. Upon excitation, **1,6-1** also shows a larger dipole moment change than that of **1,7-1**; the dipole moments of both compounds have been estimated using the Lippert–Mataga equation. The results offer the potential for synthesizing 1,6-disubstituted perylene bisimide derivatives with extended optical and electrochemical properties. Working toward their applications on *n*-type organic semiconductors (**1,6-3** and **1,7-3**) and organic photovoltaic devices (**1,6-1** and **1,7-1**) is in progress.

Acknowledgment

We thank the National Science Council (No. NSC 101-2113-M-035-001-MY2) for the financial support.

Supplementary data

Supplementary data associated with this article can be found, in the online version, at <http://dx.doi.org/10.1016/j.tetlet.2013.12.041>.

References and notes

- (a) Kaur, B.; Bhattacharya, S. N.; Henry, D. J. *Dyes Pigm.* **2013**, *99*, 502; (b) Cui, Y.; Wu, Y.; Liu, Y.; Yang, G.; Liu, L.; Fu, H.; Li, Z.; Wang, S.; Wang, Z.; Chen, Y. *Dyes Pigm.* **2013**, *97*, 129; (c) Boobalan, G.; Imran, P. S.; Nagarajan, S. *Chin. Chem. Lett.* **2012**, *23*, 149; (d) Kaur, B.; Quazi, N.; Ivanov, I.; Bhattacharya, S. N. *Dyes Pigm.* **2012**, *92*, 1108; (e) Liang, Y.; Wang, H.; Wang, D.; Liu, H.; Feng, S. *Dyes Pigm.* **2012**, *95*, 260; (f) Huang, C.; Barlow, S.; Marder, S. R. *J. Org. Chem.* **2011**, *76*, 2386; (g) Naveenraj, S.; Raj, M. R.; Anandan, S. *Dyes Pigm.* **2012**, *94*, 330; (h) Wang, R.; Shi, Z.; Zhang, C.; Zhang, A.; Chen, J.; Guo, W.; Sun, Z. *Dyes Pigm.* **2013**, *98*, 450; (i) Langhals, H.; Kirner, S. *Eur. J. Org. Chem.* **2000**, *2*, 365; (j) Nia, A. S.; Enders, C.; Binder, W. H. *Tetrahedron* **2012**, *68*, 722; (k) Bagui, M.; Dutta, T.; Zhong, H.; Li, S.; Chakraborty, S.; Keightley, A.; Peng, Z. *Tetrahedron* **2012**, *68*, 2806; (l) Kodama, K.; Kobayashi, A.; Hirose, T. *Tetrahedron Lett.* **2013**, *54*, 5514; (m) Zhang, L.; Wang, Y.; Yu, J.; Zhang, G.; Cai, X.; Wu, Y.; Wang, L. *Tetrahedron Lett.* **2013**, *54*, 4019; (n) Rajan, Y. C.; Shellaiah, M.; Huang, C.-T.; Lin, H.-C. *Tetrahedron* **2012**, *68*, 7926.
- (a) Tian, H.; Liu, P.-H.; Zhu, W.; Gao, E.; Wu, D.-J.; Cai, S. *J. Mater. Chem.* **2010**, *10*, 2708; (b) Kozma, E.; Catellani, M. *Dyes Pigm.* **2013**, *98*, 160; (c) Wang, H.-Y.; Peng, B.; Wei, W. *Prog. Chem.* **2008**, *20*, 1751; (d) Kozma, E.; Kotowski, D.; Catellani, M.; Luzzati, S.; Famulari, A.; Bertini, F. *Dyes Pigm.* **2013**, *99*, 329; (e) Dinçalp, H.; Aşkar, Z.; Zafer, C.; İcli, S. *Dyes Pigm.* **2011**, *91*, 182.
- (a) Damaceanu, M.-D.; Constantin, C.-P.; Bruma, N.; Pintea, M. *Dyes Pigm.* **2013**, *99*, 228; (b) Lucenti, E.; Botta, C.; Cariati, E.; Righetto, S.; Scarpellini, M.; Tordin, E.; Ugo, R. *Dyes Pigm.* **2013**, *96*, 748; (c) Ventura, B.; Langhals, H.; Böck, B.; Flamigni, L. *Chem. Commun.* **2012**, *48*, 4226.
- (a) Jones, B. A.; Ahrens, M. J.; Yoon, M. H.; Facchetti, A.; Marks, T. J.; Wasielewski, M. R. *Angew. Chem., Int. Ed.* **2004**, *43*, 6363; (b) Würthner, F.; Stolte, M. *Chem. Commun.* **2011**, *47*, 5109; (c) You, C.-C.; Saha-Möller, C. R.; Würthner, F. *Chem. Commun.* **2004**, *18*, 2030; (d) Hua, J.; Meng, F.; Ding, F.; Li, F.; Tian, H. *J. Mater. Chem.* **2004**, *14*, 1849.
- Givishi, R.; Reisfeld, R.; Burstein, Z. *Chem. Phys. Lett.* **1993**, *213*, 338.
- Belfield, K. D.; Bondar, M. V.; Hernandez, F. E.; Przhonska, O. V. *J. Phys. Chem. C* **2008**, *112*, 5618.
- (a) Sakong, C.; Kim, Y. D.; Choi, J.-H.; Yoon, C.; Kim, J. P. *Dyes Pigm.* **2011**, *88*, 166; (b) Choi, J.; Lee, W.; Sakong, C.; Yuk, S. B.; Park, J. S.; Kim, J. P. *Dyes Pigm.* **2012**, *94*, 34.
- Rybchinski, B.; Sinks, L. E.; Wasielewski, M. R. *J. Am. Chem. Soc.* **2004**, *126*, 12268.
- Law, K. Y. *Chem. Rev.* **1993**, *93*, 449.
- (a) Berberich, M.; Krause, A. M.; Orlandi, M.; Scandola, F.; Würthner, F. *Angew. Chem., Int. Ed.* **2008**, *47*, 6616; (b) Tan, W.; Li, X.; Zhang, J.; Tian, H. *Dyes Pigm.* **2011**, *89*, 260.
- Guo, X.; Zhang, D.; Zhu, D. *Adv. Mater.* **2004**, *16*, 125.
- Wilson, T. M.; Tauber, M. J.; Wasielewski, M. R. *J. Am. Chem. Soc.* **2009**, *131*, 8952.
- (a) Wasielewski, M. R. *Acc. Chem. Res.* **2009**, *42*, 1910; (b) Würthner, F. *Chem. Commun.* **2004**, *14*, 1564.
- (a) Fan, L.; Xu, Y.; Tian, H. *Tetrahedron Lett.* **2005**, *46*, 4443; (b) Rajasingh, P.; Cohen, R.; Shirman, E.; Shimon, L. J. W.; Rybchinski, B. *J. Org. Chem.* **2007**, *72*, 5973.
- (a) Ma, Y. S.; Wang, C. H.; Zhao, Y. J.; Yu, Y.; Han, C. X.; Qiu, X. J.; Shi, Z. *Supramol. Chem.* **2007**, *19*, 141; (b) Zhao, Y.; Wasielewski, M. R. *Tetrahedron Lett.* **1999**, *40*, 7047.

Table 3
Calculated and experimental parameters for perylene bisimide derivatives

Compound	HOMO ^a	LUMO ^a	E_g ^a	E_g ^b	Twisting angle (°)
1,6-1	-5.43	-3.03	2.40	2.13	20.09, 20.10
1,7-1	-5.33	-3.05	2.28	2.11	19.20, 19.38
2	-5.62	-3.21	2.41	2.24	9.18, 17.46
1,6-3	-6.55	-4.07	2.48	2.40	17.22, 17.34
1,7-3	-6.57	-4.11	2.46	2.40	17.02, 17.12
4	-6.25	-3.84	2.41	2.39	7.89, 15.87
5	-5.94	-3.46	2.48	2.38	0.00, 0.00

^a Calculated by DFT/B3LYP (in eV).

^b At absorption maxima ($E_g = 1240/\lambda_{max}$, in eV).

16. Wang, H.; Kaiser, T. E.; Uemura, S.; Würthner, F. *Chem. Commun.* **2008**, *10*, 1181.
17. (a) Chen, K.-Y.; Fang, T.-C.; Chang, M.-J. *Dyes Pigm.* **2011**, *92*, 517; (b) Tsai, H.-Y.; Chen, K.-Y. *Dyes Pigm.* **2013**, *96*, 319.
18. (a) Dincalp, H.; Kizilok, S.; İcli, S. *Dyes Pigm.* **2010**, *86*, 32; (b) Ren, H.; Li, J.; Zhang, T.; Wang, R.; Gao, Z.; Liu, D. *Dyes Pigm.* **2011**, *91*, 298; (c) Zhang, X.; Pang, S.; Zhang, Z.; Ding, X.; Zhang, S.; He, S.; Zhan, C. *Tetrahedron Lett.* **2012**, *53*, 1094; (d) Feng, J.; Wang, D.; Wang, S.; Zhang, L.; Li, X. *Dyes Pigm.* **2011**, *89*, 23.
19. Fin, A.; Petkova, I.; Doval, D. A.; Sakai, N.; Vauthey, E.; Matile, S. *Org. Biomol. Chem.* **2011**, *9*, 8246.
20. (a) Chao, C.-C.; Leung, M.-K. *J. Org. Chem.* **2005**, *70*, 4323; (b) Miasojedovasa, A.; Kazlauskasa, K.; Armonaita, G.; Sivamurugan, V.; Valiyaveettil, S.; Grazulevicius, J. V.; Jurseenasa, S. *Dyes Pigm.* **2012**, *92*, 1285.
21. Dhokane, B.; Gautam, P.; Misra, R. *Tetrahedron Lett.* **2012**, *53*, 2352.
22. Handa, N. V.; Mendoza, K. D.; Shirtcliff, L. D. *Org. Lett.* **2011**, *13*, 4724.
23. (a) Yuan, Z.; Li, J.; Xiao, Y.; Li, Z.; Qian, X. *J. Org. Chem.* **2010**, *75*, 3007; (b) Li, Y.; Tan, L.; Wang, Z.; Qian, H.; Shi, Y.; Hu, W. *Org. Lett.* **2008**, *10*, 529.
24. Dey, S.; Efimov, A.; Lemmettyinen, H. *Eur. J. Org. Chem.* **2011**, *30*, 5955.
25. Jones, B. A.; Facchetti, A.; Wasielewski, M. R.; Marks, T. J. *J. Am. Chem. Soc.* **2007**, *129*, 15259.
26. (a) Chen, K.-Y.; Chow, T. J. *Tetrahedron Lett.* **2010**, *51*, 5959; (b) Chen, Z.-J.; Wang, L.-M.; Zou, G.; Zhang, L.; Zhang, G.-J.; Cai, X.-F.; Teng, M.-S. *Dyes Pigm.* **2012**, *94*, 410; (c) Kong, X.; Gao, J.; Ma, T.; Wang, M.; Zhang, A.; Shi, Z.; Wei, Y. *Dyes Pigm.* **2012**, *95*, 450.
27. (a) Sun, B.; Zhao, Y.; Qiu, X.; Han, C.; Yu, Y.; Shi, Z. *Supramol. Chem.* **2008**, *20*, 537; (b) Luo, M.-H.; Chen, K.-Y. *Dyes Pigm.* **2013**, *99*, 456; (c) Würthner, F.; Stepanenko, V.; Chen, Z.; Saha-Möller, C. R.; Kocher, N.; Stalke, D. *J. Org. Chem.* **2004**, *69*, 7933; (d) Kang, H.; Jiang, W.; Wang, Z. *Dyes Pigm.* **2013**, *97*, 244.
28. Dubey, R. K.; Efimov, A.; Lemmettyinen, H. *Chem. Mater.* **2011**, *23*, 778.
29. General procedure for nitration: Compound **5** (1.8 mmol), cerium (IV) ammonium nitrate (CAN) (4.8 g, 8.8 mmol), nitric acid (8.0 g, 131.1 mmol) and dichloromethane (250 ml) were stirred at 25 °C under N₂ for 48 h. The mixture was neutralized with 10% KOH and extracted with CH₂Cl₂. After the solvent was removed, the crude product was purified by silica gel column chromatography with eluent CH₂Cl₂ to afford a mixture of 1,7- and 1,6-dinitroperylene bisimides, and ¹H NMR (500 MHz) analysis revealed a 3:1 ratio. Separation of the 1,6 and 1,7 isomers was performed on a preparative HPLC system equipped with a refractive index detector and fitted with a macro-HPLC column (Si, 8 μm, 250 × 22 mm). The eluent was 8:1 hexane/ethyl acetate flowing at 12 mL/min. Two fractions were collected from the column; the first was pure 1,6 isomer, and the second was pure 1,7 isomer. Characterization data: **1,6-3**: ¹H NMR (500 MHz, CDCl₃) δ 8.78 (s, 2H), 8.63 (d, J = 8.0 Hz, 2H), 8.30 (d, J = 8.0 Hz, 2H), 5.02 (m, 2H), 2.52 (m, 4H), 1.90 (m, 4H), 1.74 (m, 6H), 1.46 (m, 4H), 1.36 (m, 2H); MS (FAB): m/z (relative intensity) 645 (M+H⁺, 100); HRMS calcd. for C₃₆H₂₉O₈N₄ 645.1985, found 645.1983. Selected data for **1,7-3**: ¹H NMR (500 MHz, CDCl₃) δ 8.78 (s, 2H), 8.68 (d, J = 8.5 Hz, 2H), 8.28 (d, J = 8.5 Hz, 2H), 5.01 (m, 2H), 2.51 (m, 4H), 1.92 (m, 4H), 1.74 (m, 6H), 1.46 (m, 4H), 1.36 (m, 2H); MS (FAB): m/z (relative intensity) 645 (M+H⁺, 100); HRMS calcd for C₃₆H₂₉O₈N₄ 645.1985, found 645.1981.
30. General procedure for reduction: Tin chloride dihydrate (1.0 g, 4.8 mmol) and 1,6- or 1,7-dinitroperylene bisimides (0.5 g, 0.8 mmol) were suspended in 50 ml of THF, and stirred at 25 °C under N₂ for 20 min. The solvent was refluxed 80 °C with stirring for 6 h. THF is removed at the rotary evaporator, and the residue was dissolved in ethyl acetate and washed with 10% sodium hydrate solution and brine. The organic layer was dried over anhydrous MgSO₄ and the filtrate was concentrated under reduced pressure. The crude product was purified by silica gel column chromatography with eluent ethyl acetate/n-hexane (4/5) to afford 1,6- or 1,7-diaminoperylene bisimides (**1,6-1** or **1,7-1**) in 82% yield. Characterization data: **1,6-1**: ¹H NMR (400 MHz, CDCl₃) δ 8.76 (d, J = 8.4 Hz, 2H), 8.64 (d, J = 8.4 Hz, 2H), 7.88 (s, 2H), 5.05, (m, 2H), 4.98 (s, 4H), 2.59 (m, 4H), 1.92 (m, 4H), 1.76 (m, 6H), 1.27–1.56 (m, 6H); MS (FAB): m/z (relative intensity) 585 (M+H⁺, 100); HRMS calcd for C₃₆H₃₃O₄N₄ 585.2502, found 585.2508. Selected data for **1,7-1**: ¹H NMR (400 MHz, CDCl₃) δ 8.86 (d, J = 8.4 Hz, 2H), 8.42 (d, J = 8.4 Hz, 2H), 8.13 (s, 2H), 5.04, (m, 2H), 4.94 (s, 4H), 2.61 (m, 4H), 1.93 (m, 4H), 1.74 (m, 6H), 1.36–1.54 (m, 6H); MS (FAB): m/z (relative intensity) 585 (M+H⁺, 100); HRMS calcd for C₃₆H₃₃O₄N₄ 585.2502, found 585.2504.
31. Ahrens, M. J.; Tauber, M. J.; Wasielewski, M. R. *J. Org. Chem.* **2006**, *71*, 2107.
32. Lakowicz, J. R. *Principles of Fluorescence Spectroscopy*, 2nd ed.; Kluwer Academic/Plenum Publishers: New York, 1999.
33. (a) Gong, Y.; Guo, X.; Wang, S.; Su, H.; Xia, A. *J. Phys. Chem. A.* **2007**, *111*, 5806; (b) Piet, J. J.; Schuddeboom, W.; Wegewijs, B. R.; Grozema, F. C.; Warman, J. M. *J. Am. Chem. Soc.* **2001**, *123*, 5337.